Measurement of the ω meson parameters with CMD-2 detector*

R.R. Akhmetshin[a], E.V. Anashkin[a], M. Arpagaus[a], V.M. Aulchenko[a], V.Sh. Banzarov[a], L.M. Barkov[a], S.E. Baru[a], N.S. Bashtovoy[a], A.E. Bondar[a], D.V. Bondarev[a], A.V. Bragin[a], D.V. Chernyak[a], A.G. Chertovskikh[a], A.S. Dvoretsky[a], S.I. Eidelman[a], G.V. Fedotovitch[a], N.I. Gabyshev[a], A.A. Grebeniuk[a], D.N. Grigoriev[a], P.M. Ivanov[a], S.V. Karpov[a], B.I. Khazin[a], I.A. Koop[a], L.M. Kurdadze[a], A.S. Kuzmin[a], I.B. Logashenko[a], P.A. Lukin[a], K.Yu. Mikhailov[a], I.N. Nesterenko[a], V.S. Okhapkin[a], E.A. Perevedentsev[a], A.S. Popov[a], T.A. Purlatz[a], N.I. Root[a], A.A. Ruban[a], N.M. Ryskulov[a], A.G. Shamov[a], Yu.M. Shatunov[a], A.I. Shekhtman[a], B.A. Shwartz[a], V.A. Sidorov[a], A.N. Skrinsky[a], V.P. Smakhtin[a], I.G. Snopkov[a], E.P. Solodov[a], P.Yu. Stepanov[a], A.I. Sukhanov[a], J.A. Thompson[b], V.M. Titov[a], Yu.V. Yudin[a], S.G. Zverev[a]

[a] *Budker Institute of Nuclear Physics, Novosibirsk.*

[b] *University of Pittsburgh, Pittsburgh, PA 15260, USA.*

A measurement of the ω meson parameters has been performed using a data sample of about 12000 of $\omega \to \pi^+\pi^-\pi^0$ decays collected by the CMD-2 detector. The parameters of the ω resonance has been obtained: $\Gamma_{e^+e^-} = (0.605 \pm 0.014 \pm 0.010)$ keV, $\Gamma_{tot} = (8.68 \pm 0.23 \pm 0.10)$ MeV, $m_\omega = (782.71 \pm 0.07 \pm 0.04)$ MeV. Beam energy stability during the experiment has been thoroughly investigated including the analysis of the collinear tracks momenta.

1. Introduction

High precision measurements of the ω meson parameters provide valuable information for testing of various theoretical models describing interactions of light quarks. This paper presents a precise determination of the mass, total width and leptonic width of the ω, based on its dominant decay mode, $\omega \to \pi^+\pi^-\pi^0$.

The data sample was collected with the CMD-2 detector in 1994-1995 while scanning the center of mass energy range $2E_{beam}$ from 780 to 810 MeV at the VEPP-2M collider [1]. The resonant depolarization method [2] was used for precise beam energy calibration at each point. The collected integrated luminosity of 141 nb^{-1} corresponds to $\sim 7 \times 10^4$ ω meson decays.

2. Analysis

The ω meson parameters were measured by the $\omega \to \pi^+\pi^-\pi^0$ decay mode.

For analysis events with two tracks originating from the same vertex, each with a polar angle $0.85 < \theta < \pi - 0.85$ within the fiducial volume of the detector, were selected for further analysis.

Only DC information has been used for the selection of 3π events to minimize systematic error of the registration efficiency. Most of the background comes from the processes with a hard photon emission:

$$e^+e^- \to e^+e^-\gamma,\ \pi^+\pi^-\gamma,\ \mu^+\mu^-\gamma.$$

These processes have the same signature as $\pi^+\pi^-\pi^0$, except for a very different acollinearity angle ($\Delta\phi = \pi - |\varphi_1 - \varphi_2|$) distribution peaked near $\Delta\phi = 0$. Thus, the rejection of events with a small $\Delta\phi$ drastically reduces the background, at the same time decreasing the number of 3π events. A value of $\Delta\phi = 0.25$ was used as a reasonable compromise (see Fig. 1-a).

Additional background suppression can be achieved using the "missing mass" parameter, assuming charged particles to be pions and taking into account energy-momentum conservation. For real $\pi^+\pi^-\pi^0$ events the distribution of the missing mass squared has a peak in the region of $M^2_{\pi^0}$ in contrast to the background processes which have a peak around zero for $e^+e^- \to \pi^+\pi^-(\gamma)$, $\mu^+\mu^-(\gamma)$ or in the negative region for $e^+e^- \to e^+e^-(\gamma)$. Figure 1-b shows the squared missing mass of two charged particles versus maximum energy deposition of these two particles in the calorimeter. The lines show the cut applied for the separation of $\pi^+\pi^-\pi^0$ events from the background.

The number of $\pi^+\pi^-\pi^0$ events was obtained in two different ways. The first one is to fit the histograms of the $\pi^+\pi^-$ missing mass with the sum of Gaussian functions describing 3π and background events. The second one is to reject the cosmic and beam background by fitting the distribution of the z-coordinate of the vertex with the Gaussian function and the constant background. In the last case remaining events $e^+e^- \to e^+e^-(\gamma)$, $\pi^+\pi^-(\gamma)$, $\mu^+\mu^-(\gamma)$ were simulated and subtracted from the total number of events at each point according to the correspond-

*This work is supported in part by the Russian Foundation for Basic Research under grant RFBR-98-02-17851 and the US DOE grant DEFG0291ER40646.

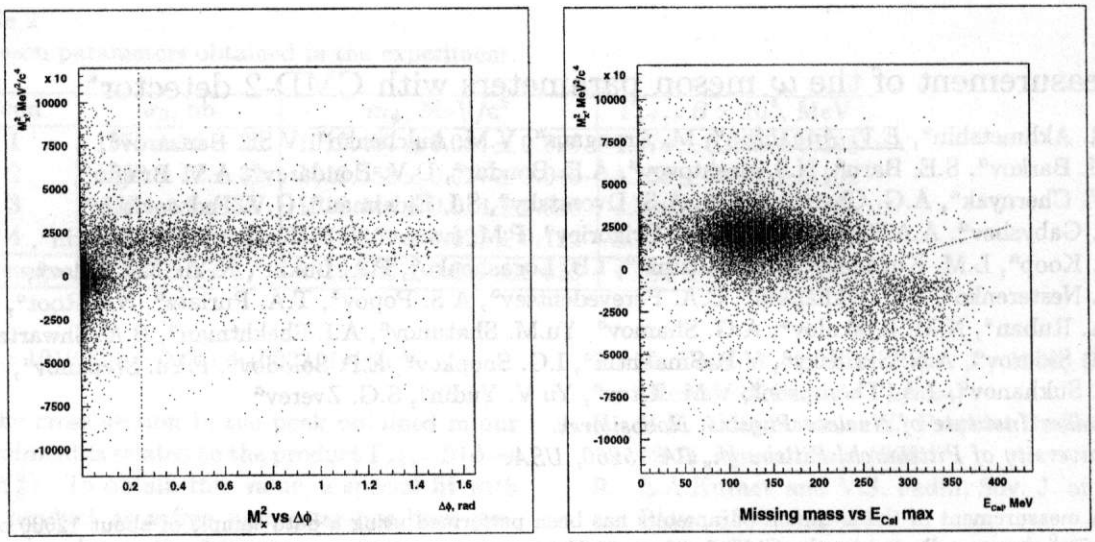

(a) (b)

Figure 1. Graphic presentation of cuts on $\Delta\phi$ (a) and M_X^2 vs E_{CsI}^{max} (b). (b) contains events after cut (a). In Fig. (b) the lower right corner corresponds to rejected events

ing integrated luminosity. Both approaches give the same result within the statistical errors.

At each energy the cross section of $\pi^+\pi^-\pi^0$ production was calculated according to the formula:

$$\sigma = \frac{N_{\pi^+\pi^-\pi^0}}{L \cdot \varepsilon_{trig} \cdot \varepsilon_{MC} \cdot \varepsilon_{M_X^2} \cdot (1+\delta_{rad}) \cdot (1+\delta_E)},$$

where $N_{\pi^+\pi^-\pi^0}$ is the number of events; L is the integrated luminosity determined from large angle Bhabha events with the help of the procedure described in [3]; δ_{rad} is the radiative correction calculated according to [4] with an accuracy better than 0.5%; ε_{trig}, ε_{MC}, $\varepsilon_{M_X^2}$ are trigger efficiency, geometrical efficiency (acceptance) multiplied by the reconstruction efficiency, and efficiency of the cut shown in Fig. 1-b respectively. The acceptance is the probability to detect two pions from the ω decay within a given solid angle. It was calculated by MC taking into account radiative photons emitted by the primary particles.

The efficiencies ε_{MC} and $\varepsilon_{M_X^2}$ were calculated by Monte Carlo simulation. Their systematic errors were estimated with the help of special "test" events obtained as a result of the constraint fit based on the information from the ZC and CsI calorimeter only. About 40% of the $\pi^+\pi^-\pi^0$ events have two clusters in the CsI calorimeter resulting from a neutral pion decay. Using the polar and azimuthal angles of these clusters as well as the hits of charged tracks in ZC, one can reconstruct the $\omega \to \pi^+\pi^-\pi^0$ event without DC information. "Test" events were also used to determine the trigger efficiency.

Typical values of the efficiencies and corrections are presented in Table 1 for $2E_{beam} =$ 782.0 MeV (the ω meson peak).

The beam energy at each point was measured by the resonant depolarization method [2]. The integrated luminosity, radiative correction, number of 3π events and cross section for $e^+e^- \to \omega \to \pi^+\pi^-\pi^0$ at each energy are presented in Table 2.

Experimental data were fitted with a function which includes the interference of the ω and ϕ mesons and non-resonant background:

$$\sigma_{3\pi}(s) = \frac{F_{3\pi}(s)}{s^{3/2}} \cdot |A_\omega + e^{i\alpha} A_\phi + A_{bg}|^2, \qquad (1)$$

$$\begin{aligned}
A_V &= \frac{m_V^2 \Gamma_V \sqrt{\sigma_V m_V / F_{3\pi}(m_V^2)}}{s - m_V^2 + i\sqrt{s}\Gamma_V(s)}, \\
A_{bg} &= m_\omega^{3/2} \sqrt{\sigma_{bg}/F_{3\pi}(m_\omega^2)}, \\
\Gamma_\omega(s) &= \Gamma_\omega \cdot \Big(Br_{\pi^+\pi^-} \frac{m_\omega^2 F_{2\pi}(s)}{s F_{2\pi}(m_\omega^2)} + \\
&\quad Br_{\pi^0\gamma} \frac{F_{\pi^0\gamma}(s)}{F_{\pi^0\gamma}(m_\omega^2)} + Br_{3\pi} \frac{\sqrt{s} F_{3\pi}(s)}{m_\omega F_{3\pi}(m_\omega^2)} \Big), \\
F_{\pi^0\gamma}(s) &= (\sqrt{s}(1 - m_{\pi^0}^2/s))^3, \\
F_{2\pi}(s) &= (s/4 - m_\pi^2)^{3/2},
\end{aligned}$$

where m_V, Γ_V, σ_V are mass, width and peak cross section ($s = m_V^2$) for the vector meson ω or ϕ, α is a relative phase of $\omega - \phi$ mixing taken

to be $(155 \pm 15)^\circ$ according to [5], , $F_{3\pi}(s)$ is a smooth function which describes the dynamics of $V \to \pi^+\pi^-\pi^0$ decay including the phase space. It was numerically calculated assuming the model of the $V \to \rho\pi \to \pi^+\pi^-\pi^0$ decay. $\Gamma_\phi(s)$ has been described in a similar manner to ω using appropriate branchings and phase space factors [7].

Table 1
Efficiencies, corrections and their errors at $2E_{beam} = 782.0$ MeV

Efficiency	Value, %	Stat. err., %	Sys. err., %
ε_{MC}	19.0	0.1	0.1
ε_{trig}	99.5	0.2	0.1
$\varepsilon_{M_X^2}$	99.2	0.2	0.2
$1+\delta_{rad}$	78.5	0.1	0.5

Table 2
Integrated luminosity, radiative corrections and cross section for $e^+e^- \to \pi^+\pi^-\pi^0$

E_{beam}, MeV	$\int Ldt$, nb^{-1}	δ_{rad}	$\sigma(\omega \to \pi^+\pi^-\pi^0)$, nb
380.092	6.10±0.10	-0.183	68±11
382.083	10.61±0.14	-0.191	70±8
385.053	8.09±0.12	-0.206	178±15
387.190	6.39±0.11	-0.220	277±21
389.087	6.51±0.11	-0.232	784±40
390.087	6.91±0.11	-0.232	1185±50
391.113	18.71±0.18	-0.215	1480±30
392.119	10.26±0.14	-0.172	1328±44
393.018	5.08±0.09	-0.116	897±43
395.047	9.15±0.12	0.031	414±19
397.068	9.02±0.08	0.178	195±11
400.000	9.59±0.12	0.358	126±8
405.071	14.05±0.15	0.613	56±4

The cross section values were fitted by the function (1). The ω meson mass, width, peak cross section and background cross section were optimized, while ϕ meson parameters were fixed at their world average values [6].

The energy dependence of the cross section is shown in Fig. 2 (experimental points and the optimal fitting curve). The following ω meson parameters were obtained from the fit: $\sigma_0 = (1482 \pm 23)$ nb, $M_\omega = (782.71 \pm 0.08)$ MeV/c^2, $\Gamma_\omega = (8.68 \pm 0.23)$ MeV, $\sigma_{bg} = (12 \pm 5)$ nb.

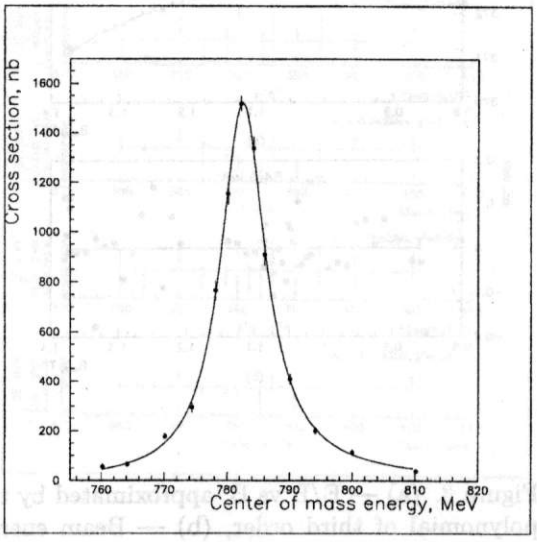

Figure 2. ω meson excitation curve

The systematic error of σ_0 is about 1.3% and comes from the following sources:

reconstruction efficiency	0.5% ;
trigger efficiency	0.1% ;
radiative corrections for the process $e^+e^- \to \pi^+\pi^-\pi^0$	0.5% ;
decays in flight	0.1% ;
pion nuclear interaction	0.2% ;
solid angle uncertainty	0.3% ;
luminosity determination	1.0% .

The systematic error of the mass was found to be about 40 keV, dominated by the stability of the beam energy.

3. Beam energy stability

One can estimate beam energy fluctuations using the depolarization data and the following ideas:

- points with several depolarization measurements at the same magnetic field but different average temperature give direct evaluation of energy-temperature dependence;
- points at different magnetic field should be on the smooth curve. The deviation from this curve can be used as if all points are at the same magnetic field value much like in a previous case.

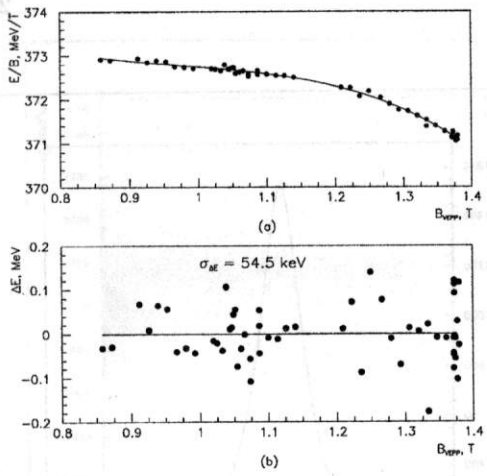

Figure 3. (a) — E/B vs B, approximated by the polynomial of third order, (b) — Beam energy deviations from (a); E — VEPP-2M beam energy, B — VEPP-2M bending magnets field

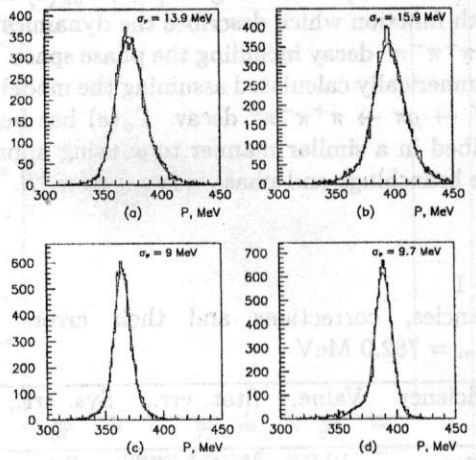

Figure 4. Momentum distribution. (a) – average momentum for $e^+e^- \to \pi^+\pi^-$, $e^+e^- \to \mu^+\mu^-$. (b) – average momentum for $e^+e^- \to e^+e^-$. (c) – one arc momentum for $e^+e^- \to \pi^+\pi^-$, $e^+e^- \to \mu^+\mu^-$. (d) – one arc momentum for $e^+e^- \to e^+e^-$. All distributions are fitted with the function described by (3)

Fig. 3 illustrates the second case with the VEPP-2M depolarization data of **PHI-94** and **RHOM-95** runs.

The tracking system of the CMD-2 allows to control independently beam energy stability during data taking by the measuring of the collinear tracks momenta. This technique can be used anywhere in the energy range of VEPP-2M since it uses processes $e^+e^- \to e^+e^-$, $e^+e^- \to \mu^+\mu^-$ and $e^+e^- \to \pi^+\pi^-$.

Event collinearity is defined by the DC information only. The event is considered to be collinear if the following conditions are met:

- There are exactly two tracks from the same vertex;
- Tracks belong to the particles with the opposite charges;
- Each track has at least 10 hits in the r-φ plane;
- Track impact parameter relative to the beam axis does not exceed 0.1 cm for each track;
- Absolute Z-coordinate of the vertex is less than 5 cm;
- Polar angle of the first track in the event is inside the $1 \div (\pi - 1)$ interval;
- Acollinearity of two tracks in the r-φ plane is less than 0.02;
- The acollinearity of two tracks in polar angle is less than 0.1.

The energy deposition in the barrel calorimeter was used as the only parameter to distinguish between $e^+e^- \to e^+e^-$ and other collinear events. For $e^+e^- \to e^+e^-$the following conditions should be met:

- $\min(E_{cl}) > 0.65 E_{beam}$
- $\max(E_{cl}) < 1.2 E_{beam}$

Events were selected as $e^+e^- \to \mu^+\mu^-$ or $e^+e^- \to \pi^+\pi^-$ if:

- $\sum_{i=1}^{2} E_{cl}(i) < E_{beam}$
- $\min(E_{cl}) > 50\,\mathrm{MeV}$

The last cut rejects events with one of the tracks pointing to the dead region of the calorimeter.

During the reconstruction process all collinear tracks are fitted with the single arc. The momentum corresponding to the curvature of this arc ($\widehat{p}$) has the accuracy 1.5–2 times better than an average momentum of two tracks (Fig. 4).

$\widehat{p}$ distribution has non-Gaussian tails mostly due to radiative photons. To get the reasonable average value of the $\widehat{p}$ two approaches have been used:

1. The distribution is fitted inside the limited range around the maximum, where it is quite close to the standard Gaussian. In that case tails have practically no influence on the average value but interval boundaries are quite arbitrary and may shift the average if changed. We use the following limits: $\left|\sqrt{\vec{p}^2+m_e^2}-E_{beam}\right| < 10\,\text{MeV}$ for $e^+e^- \to e^+e^-$ and $\left|\sqrt{\vec{p}^2+m_\pi^2}-E_{beam}\right| < 10\,\text{MeV}$ for $e^+e^- \to \pi^+\pi^-$, $e^+e^- \to \mu^+\mu^-$.

2. The distribution is fitted with the asymmetrical function. For this purpose we use Gram-Charlier approximation series [14], described by:

$$f(z) = \frac{A}{\sqrt{2\pi}} e^{-\frac{z^2}{2}} \left[1 + \frac{\gamma_1}{6}\left(z^3 - 3z\right) + \frac{\gamma_2}{24}\left(z^4 - 6z^2 + 3\right)\right], \quad (2)$$

$$z = \frac{x - x_0}{\sigma},$$

where $A, x_0, \sigma, \gamma_1, \gamma_2$ are parameters of the fit. Note, that for $\gamma_1 = \gamma_2 = 0$ this distribution becomes standard Gaussian and $\int_{-\infty}^{\infty} f(z)dz = A$ for all γ_1, γ_2. Comparing with the first approach we have more fit parameters, but now the result is independent of the interval boundaries and so they were significantly extended: $\left|\sqrt{\vec{p}^2+m_e^2}-E_{beam}\right| < 20\,\text{MeV}$ for $e^+e^- \to e^+e^-$ and $\left|\sqrt{\vec{p}^2+m_\pi^2}-E_{beam}\right| < 20\,\text{MeV}$ for $e^+e^- \to \pi^+\pi^-$, $e^+e^- \to \mu^+\mu^-$.

The accuracy of the average beam energy at each point σ_E depends on the number of collinear events and on the accuracy of the momentum measurement for a single event.

The suggested technique is intended not for the absolute determination of the beam energy but for the check of the beam energy stability. So we have to control not the value of $\Delta E = \sqrt{\vec{p}^2+m^2}-E_{beam}$ itself but its dependence on the beam energy. It means that we can combine the results for both classes of event with the average value of ΔE set to an arbitrary constant, e.g. $\Delta E = 0$. In the range of the ω meson cross sections for $e^+e^- \to e^+e^-$ and processes $e^+e^- \to \pi^+\pi^-$ have the same order of magnitude and their integration can significantly improve the accuracy.

Both approaches give approximately the same result, demonstrated in Fig. 5.

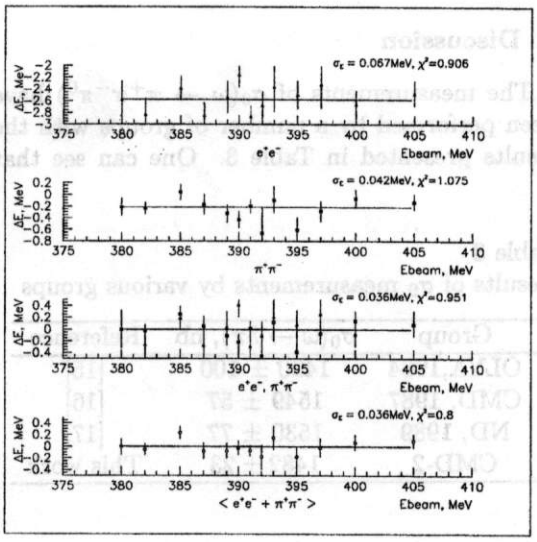

Figure 5. Beam energy stability. From up to down: ΔE for the $e^+e^- \to e^+e^-$ event class, ΔE for the $e^+e^- \to \pi^+\pi^-$ event class, both classes on the same plot with the ΔE set to 0 and the combined result

4. Estimation of the possible error of the ω meson mass

Temperature drift.
Depolarization data in the ω meson range do not show any clear dependence of the beam energy on the VEPP-2M average temperature, but as a reasonable upper limit one can use the dependence in the ϕ meson range. Given the temperature fluctuation about 1°C (r.m.s.) the following estimation can be made:

$$\sigma_T \sim 1^\circ\text{C} \Longrightarrow \sigma_\text{E} < 30\ \text{keV} \Longrightarrow \sigma_{\text{m}_\omega} < \frac{2\sigma_\text{E}}{\sqrt{\text{n}}} \approx 15\ \text{keV},$$

where n = 13 is the number of energy points.

Long-time stability of the beam energy. Based on the deviation of the depolarization data from the E_{beam}/B dependence curve (Fig. 3) we estimate the long-time stability of the VEPP-2M beam energy being of the order of 50 keV. Thus:

$$\sigma_E \approx 50\ \text{keV} \Longrightarrow \sigma_{\text{m}_\omega} < \frac{2\sigma_\text{E}}{\sqrt{\text{n}}} \approx 25\ \text{keV}$$

Momentum measurement for collinear events. Finally, direct measurements of the collinear events momenta suggest that VEPP-2M beam energy instability cannot exceed 150 keV. From this:

$$\sigma_E \sim 150\ \text{keV} \Longrightarrow \sigma_{\text{m}_\omega} < \frac{2\sigma_\text{E}}{\sqrt{\text{n}}} \approx 75\ \text{keV}$$

5. Discussion

The measurements of $\sigma_0(\omega \to \pi^+\pi^-\pi^0)$ have been performed by a number of groups with the results presented in Table 3. One can see that

Table 3
Results of σ_0 measurements by various groups

Group	$\sigma_0(\omega \to 3\pi)$, nb	Reference
OLYA,1984	1420 ± 100	[15]
CMD, 1987	1549 ± 57	[16]
ND, 1989	1530 ± 77	[17]
CMD-2	1482 ± 23	This work

our value $\sigma_0(\omega \to \pi^+\pi^-\pi^0) = (1482 \pm 23)$ nb does not contradict these measurements and is the most precise.

The cross section in the peak obtained in our experiment is related to the product $\Gamma_{e^+e^-}\cdot\mathrm{Br}(\omega \to 3\pi)$. To obtain this value, the fit with this product as a free parameter have been performed with the following result:

$$\Gamma_{e^+e^-} \cdot \mathrm{Br}(\omega \to 3\pi) = (0.537 \pm 0.012 \pm 0.009)\,\mathrm{keV},$$

which is the most precise direct measurement. Using $\Gamma_{e^+e^-}$ from other experiments, one can obtain $Br(\omega \to 3\pi)$, according to the next formula:

$$Br(\omega \to 3\pi) = \sigma_0(\omega \to 3\pi) \cdot \frac{\Gamma_\omega}{\Gamma_{e^+e^-}} \cdot \frac{M_\omega^2}{12\pi}.$$

For example, for $\Gamma_{e^+e^-} = (0.60 \pm 0.02)$ keV from [6], $Br(\omega \to 3\pi) = 0.895 \pm 0.006 \pm 0.010$ can be obtained. Alternatively, taking $Br(\omega \to 3\pi)$ from other works, $\Gamma_{e^+e^-}$ can be calculated. For $Br(\omega \to 3\pi) = 0.888 \pm 0.007$ from [6], we obtain for the leptonic width $\Gamma_{e^+e^-} = (0.605 \pm 0.014 \pm 0.010)$ keV.

Figure 6 shows results of previous measurements on the ω meson mass. Hereafter CMD95 marks results of this work. The left shaded bar corresponds to the current world average. This value is dominated by the CMD87 experiment which has claimed the accuracy far better than all other experiments.

The CMD87 experiment used the same resonant depolarization method (RDM) as our experiment. However, since the time of CMD87 the upgrade of VEPP-2M collider has been done. Much better understanding of the implementation of the RDM technique has appeared and upgrade of the corresponding hardware has been done too. In our experiment the beam was polarized in the booster ring since it requires as high energy of

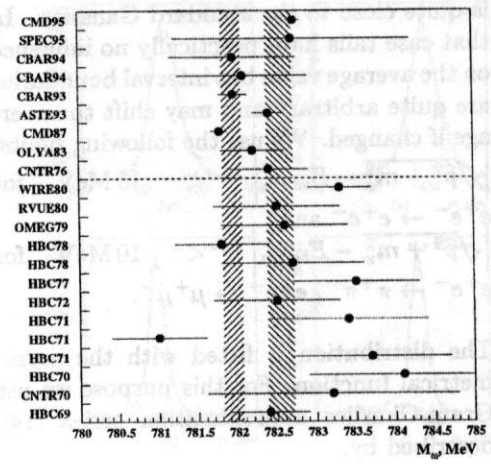

Figure 6. Experimental data on the ω meson mass. The left shaded bar corresponds to the current world average [6], the right one — to the world average before the CMD87 experiment. This work (CMD95) and experiments below the dashed line are not used for the current world average

the beam as possible to minimize the polarization time. Parameters of VEPP-2M itself were not changed and RDM measurements were performed under the same conditions as data taking. In addition, the power of the depolarization generator has been reduced to the minimum required for RDM to exclude any parasitic influences.

During the CMD87 experiment the beam was polarized in the VEPP-2M ring itself at the beam energy of about 700 MeV since the booster ring did not yet exist at that time. This led to changes of the collider parameters before each RDM measurement including changes of betatron frequencies ν_x, ν_z in order to pass through intrinsic spin resonances. The imperfection resonance at the "magic energy" $E_{beam} = 440.65$ MeV was crossed adiabatically by decompensation of the longitudinal magnetic field of the detector (so called "partial siberian snake" mode [18]).

One of the parameters strongly affecting the beam energy is the collider temperature. During polarization at high energy, the collider temperature increased by approximately 10 °C and the temperature stabilization system was not intended for such strong and rapid changes of temperature. In principle, it could lead to the relative variations of the beam energy of the order of 10^{-3}.

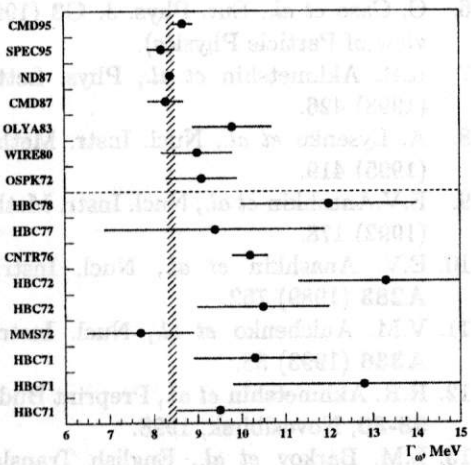

(a) ω meson total width

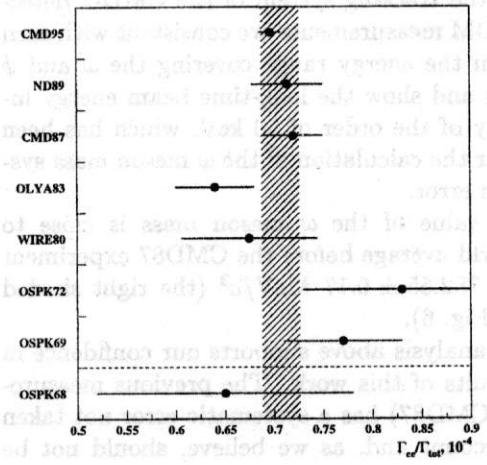

(b) Leptonic branching ratio$\Gamma_{e^+e^-}/\Gamma_\omega$

Figure 7. Experimental data on the ω meson total width (a) and leptonic branching ratio (b). Vertical shaded bars correspond to the current world averages [6]. This work (CMD95) and experiments below dashed lines are not used for averages

The depolarization generator used for CMD87 had the power of about six orders of magnitude higher than that necessary for depolarization and there was a possibility of depolarization at the parasitic side frequency originating from the interference with other electric systems of the collider.

Today, almost fifteen years after the CMD87 experiment, it is impossible to indicate the exact combination of factors which has led to considerable shift of the beam energy scale. In our experiment all mentioned sources of the systematic error in RDM were excluded and the beam energy stability during data taking has been thoroughly analysed. This analysis was based both on the deviations of about 60 RDM measurements at different energies from the predicted values and on direct measurements of the beam energy stability by the tracking system of the CMD-2 detector. RDM measurements are consistent with each other in the energy range covering the ω and ϕ mesons and show the long-time beam energy instability of the order of 50 keV, which has been used for the calculation of the ω meson mass systematic error.

Our value of the ω meson mass is close to the world average before the CMD87 experiment $M_\omega = 782.55 \pm 0.17$ MeV/c^2 (the right shaded bar in Fig. 6).

The analysis above supports our confidence in the results of this work. The previous measurement (CMD87) has a systematic error not taken into account and, as we believe, should not be averaged with the results of other experiments.

The total width of the ω meson is in good agreement with that from previous experiments (Fig. 7-a) similarly to the leptonic branching ratio $\Gamma_{e^+e^-}/\Gamma_\omega$ (Fig. 7-b).

6. Conclusion

Using the CMD-2 data sample of 1.2×10^4 $\omega \to \pi^+\pi^-\pi^0$ events, the following values of the ω meson parameters have been obtained:

$$\begin{aligned}
\sigma_0 &= (1482 \pm 23 \pm 25)\,\text{nb},\\
M_\omega &= (782.71 \pm 0.07 \pm 0.04)\,\text{MeV}/c^2,\\
\Gamma_\omega &= (8.68 \pm 0.23 \pm 0.10)\,\text{MeV},\\
\Gamma_{e^+e^-} &\cdot Br(\omega \to \pi^+\pi^-\pi^0) =\\
&(0.537 \pm 0.012 \pm 0.009) \cdot 10^{-3}\,\text{MeV}.
\end{aligned}$$

These results except for the total width value are more precise than the corresponding measurements from all previous experiments.

7. Acknowledgements

The authors are grateful to the staff of VEPP-2M for excellent performance of the collider, to all engineers and technicians who participated in the design, commissioning and operation of CMD-2.

REFERENCES

1. V.V. Anashin *et al.*, Preprint Budker INP **84-114**, Novosibirsk, 1984.
2. A.N. Skrinsky, Yu.M. Shatunov, Soviet Physics Uspekhi **32(6)** (1989) 548.
3. R.R. Akhmetshin *et al.*, Preprint Budker INP **99-11**, Novosibirsk, 1999.
4. E.A. Kuraev and V.S. Fadin, Sov. J. Nucl. Phys. **41** (1985) 466.
5. S.I. Dolinsky *et al.*, Phys. Rep. **202** (1991) 99.
6. C. Caso *et al.*, Eur. Phys. J. **C3** (1998) (Review of Particle Physics).
7. R.R. Akhmetshin *et al.*, Phys. Lett. **B434** (1998) 426.
8. A. Lysenko *et al.*, Nucl. Instr. Meth. **A359** (1995) 419.
9. E.V.Anashkin *et al.*, Nucl. Instr. Meth. **A323** (1992) 178.
10. E.V. Anashkin *et al.*, Nucl. Instr. Meth. **A283** (1989) 752.
11. V.M. Aulchenko *et al.*, Nucl. Instr. Meth. **A336** (1993) 53.
12. R.R. Akhmetshin *et al.*, Preprint Budker INP **98-30**, Novosibirsk, 1998.
13. L.M. Barkov *et al.*, English Translation of Sov. Phys. ZhETF Letters **46** (1987) 164.
14. G. Korn, T. Korn, Mathematical handbook. Moscow, 1977, p. 614. (In Russian).
15. L.M. Kurdadze *et al.*, Preprint Budker INP **84-7**, Novosibirsk, 1984.
16. L.M. Barkov *et al.*, Preprint Budker INP **87-95**, Novosibirsk, 1984.
17. S.I. Dolinsky *et al.*, Preprint Budker INP **89-104**, Novosibirsk, 1984.
18. Ya.S. Derbenev *et al.*, Proceedings of X International conference on charged particle colliders, Protvino, 1977.